



ELSEVIER

Contents lists available at ScienceDirect

Data in brief

journal homepage: www.elsevier.com/locate/dib

Data Article

Characterization of food waste-driven carbon dot focusing on chemical structural, electron relaxation behavior and Fe³⁺ selective sensingJungbin Ahn^{a,1}, Younghan Song^{a,1}, Ji Eon Kwon^b,
Jeongyeon Woo^a, Hyungsup Kim^{a,*}^a Department of Organic and Nano System Engineering, Konkuk University, Seoul, 05029, Republic of Korea^b Department of Materials Science and Engineering, Seoul National University, Seoul, 08826, Republic of Korea

ARTICLE INFO

Article history:

Received 13 April 2019

Received in revised form 8 May 2019

Accepted 16 May 2019

Available online 23 May 2019

Keywords:

Carbon dots

Electron relaxation behavior

Chemical structural analysis

Fe³⁺ quenching

ABSTRACT

In the study, carbon dot (CD) with high fluorescence properties was obtained via one-step hydrothermal carbonization of food model and sandwich leftover, respectively. The data in the article represent the change of the chemical structure and PL properties of the food waste-driven carbon dot (FWCDs). In higher carbonization temperature, pyridinic N and graphitic N were increased while amino N and pyrrolic N was decreased. The lifetime was increased with the increase of temperature. The CD prepared from sandwich leftover showed the dependency of the emission on the exciting wavelength and excellent Fe³⁺ sensitivity without significant change of lifetime. It also had a pH-sensitive fluorescence feature and good stability in NaCl solutions. For more insight, please see Food waste-driven N-doped carbon dots: Applications for Fe³⁺ sensing and cell imaging Ahn et al., 2019.

© 2019 The Authors. Published by Elsevier Inc. This is an open access article under the CC BY license (<http://creativecommons.org/licenses/by/4.0/>).

DOI of original article: <https://doi.org/10.1016/j.msec.2019.04.019>.

* Corresponding author.

E-mail address: iconclast@konkuk.ac.kr (H. Kim).¹ These two authors contributed equally to this work.<https://doi.org/10.1016/j.dib.2019.104038>2352-3409/© 2019 The Authors. Published by Elsevier Inc. This is an open access article under the CC BY license (<http://creativecommons.org/licenses/by/4.0/>).

Specifications table

Subject area	Physics, Chemistry, Material science
More specific subject area	Photoluminescence, Carbon-based Nanomaterial,
Type of data	Table, figure, graph, image
How data was acquired	XPS (K-alpha, Thermo Scientific), TCSPC (Fluo Time 200 instrument, Picoquant), Digital camera (G10, Canon), PL spectrometer (FS-2, SICNCO), UV spectrometer (Cary 60 UV/vis spectrophotometer, Agilent Technologies)
Data format	Raw, analyzed
Experimental factors	Carbon dots were synthesized using food wastes via one-step hydrothermal carbonization
Experimental features	Food waste-driven carbon dots were characterized with XPS, TCSPC, PL and UV spectrometer
Data source location	Seoul, Republic of Korea
Data accessibility	Physics, Chemistry, Material science
Related research article	J. Ahn, Y. Song, J. E. Kwon, S. H. Lee, K. S. Park, S. Kim, J. Woo and H. Kim, Food waste-driven N-doped carbon dots: Applications for Fe ³⁺ sensing and cell imaging, Materials Science & Engineering C 102 (2019) 106–112.

Value of the data

- This data can help for the understanding of structural change of CD during hydrothermal carbonization of complex mixture including food waste.
- The changes of the chemical structure and the electron relaxation behavior along the carbonization temperature is beneficial to study the photoluminescence mechanism of carbon dots.
- The data exhibit the possibility of the prepared carbon dot for Fe³⁺ sensing with high selectivity in the presence of other metal ion.

1. Data

Nanomaterials with fluorescence properties including carbon dots are having great attention due to its wide application area such as metal ion sensing and biological imaging [1–3]. Herein, we synthesized carbon dots with food waste-driven cat feed stock and sandwich leftover.

Fig. 1 shows the chemical structure changes of FWCDs along the carbonization temperature. As the temperature increased, the peak for –OH bonding was decreased while the peaks for C–O and C=O bonding were increased (Fig. 1a). Fig. 1b shows the ratio of each nitrogen speciation in the synthesized CDs, which indicate the structure of N-containing aromatic compounds were more developed along the temperature. The TEM images of synthesized CDs their size distribution can be seen in Fig. 1 of [1].

The Fig. 2 shows the lifetime decay curves of the CDs and were interpreted in terms of a tri-exponential function:

$$I(t) = \int_{-\infty}^t IRF(t') \sum_{i=1}^n A_i e^{-\frac{t-t'}{\tau_i}} dt' \quad (1)$$

Where A_i and τ_i are the amplitude and the decay times of lifetimes, respectively. All the curves were well-fitted with χ^2 value below 1.1.

Radiative lifetime was can be calculated from the average lifetime (τ_{av}) and the fluorescence quantum yield (ϕ) using Equation (2). The lifetime and the radiative/non-radiative recombination rate are finally obtained from the radiative and non-radiative lifetimes using Equations (3) and (4) (Table 1 of [1])

$$\phi = \frac{\tau_{av}}{\tau_r} \quad (2)$$

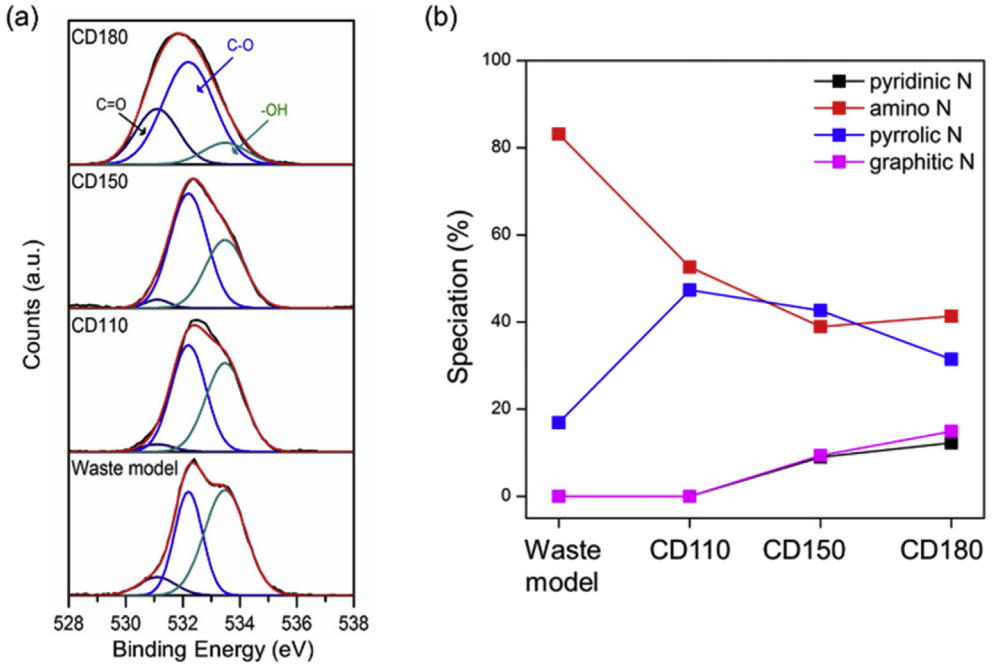


Fig. 1. (a) High resolution XPS spectra of O1s and (b) the speciation of the nitrogen bonding of the samples.

$$\frac{1}{\tau_{av}} = \frac{1}{\tau_r} + \frac{1}{\tau_{nr}} \quad (3)$$

$$k_r = \frac{1}{\tau_r}, \quad k_{nr} = \frac{1}{\tau_{nr}} \quad (4)$$

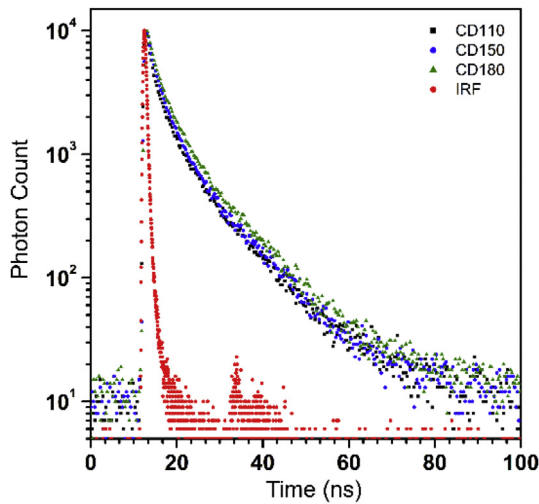


Fig. 2. Decay curves of the CDs collected at emission wavelength of the individual maximum intensity.

Table 1

Functional groups identified from FT-IR spectra of the samples.

Wavenumber (cm ⁻¹)	Types of vibration	Functional groups	References in the article
3400–3200	Stretching	-OH, -NH	[5]
2926	Asymmetrical stretching	C-H	[5]
2857	Symmetrical stretching	C-H	[5]
1657	Stretching	C=O (Amide I)	[6]
1640	Stretching	C=O	[6]
1580	Bending, stretching	-NH, -NH (Amide II)	[5,6]
1400	Stretching	C-N	[7]
1050	Stretching	C-O	[8]
872, 800	Out-of-plane bending	C-H of phenazine skeleton	[9]

where φ = fluorescence quantum yield, τ_{av} = average lifetime, τ_r = radiative lifetime, τ_{nr} = non-radiative lifetime, k_r = radiative recombination rate constant and k_{nr} = non-radiative recombination rate constant.

The functional groups of waste model and CDs were summarized in Table 1.

Fig. 3 shows the image of used sandwich leftover and PL spectra of synthesized FWCDs. The TEM images of FWCDs can be seen in Fig. 5a of [1].

The FWCDs showed the selective sensing capability for Fe³⁺. In Fig. 4a, the fluorescence intensity of FWCDs solutions was significantly decreased in the presence of Fe³⁺ while other metal ions insignificantly influenced on the PL. The quenching mechanism of FWCDs was characterized by Time-correlated single photon counting (TCSPC), UV-vis spectrometer and PL spectrometer. Fig. 4b shows the fluorescence decays of the FWCDs quenched by Fe³⁺. The obtained values were summarized in Table 2. The average lifetime of FWCDs was slightly increased in Fe³⁺ solutions. However, the lifetime decay of FWCDs in Fe³⁺ solution was not changed along Fe³⁺ concentration. The identical lifetime indicates that the energy transfer between Fe³⁺ and FWCDs did not occur in the quenching process, known as Inner Filter Effect (IFE) [4]. In Fig. 4c, the typical feature of IFE behavior was shown by the overlapping curves of the absorption band of Fe³⁺ in UV spectra and emission or excitation bands of FWCDs in PL spectra. Table 3 are the list of comparing the detection of Fe³⁺ with carbon dots prepared from various biomass-based sources. Fig. 5 exhibits the FWCDs had a pH-sensitive fluorescence feature and good stability in NaCl solutions.

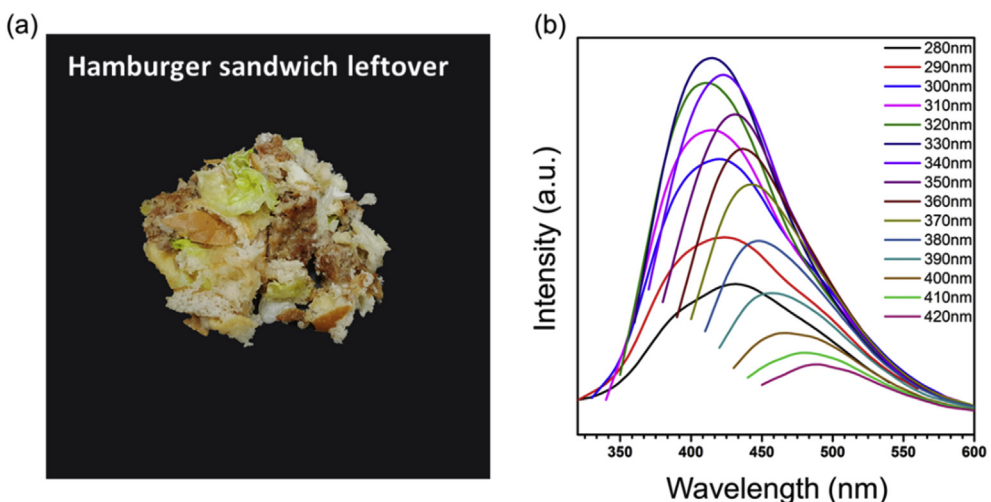


Fig. 3. (a) The digital image of precursors for FWCDs and (b) emission peaks excited by each wavelength, which indicated by individual colors.

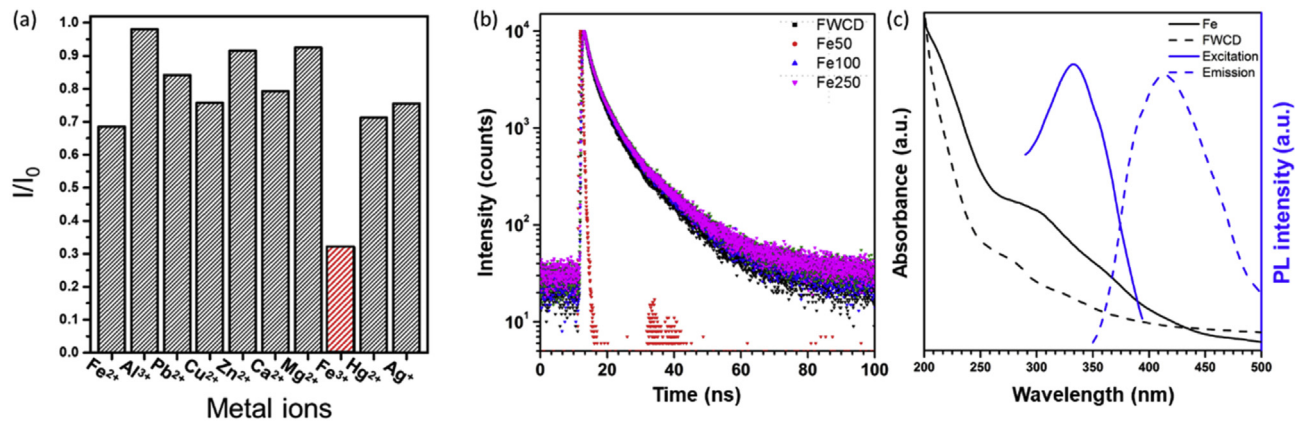


Fig. 4. (a) Plot of relative fluorescence intensity of FWCDs solution in different metal solutions. (b) Fluorescence decay curves of FWCDs in the absence and presence of Fe^{3+} under excitation of 342 nm. Fe50, Fe100 and Fe250 refer lifetime decay of FWCDs in the different Fe^{3+} concentrations of 50, 100 and 250 μM , respectively. (c) UV-vis absorption spectra of Fe^{3+} and FWCDs, and photoluminescence excitation/emission curves of FWCD.

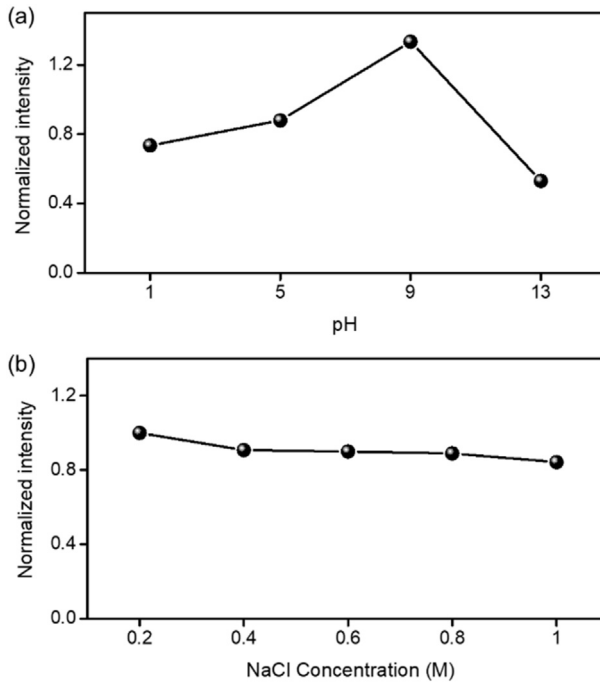


Fig. 5. The effects of different (a) pH and (b) NaCl concentrations to the fluorescence intensity of FWCDs solution.

Table 2

Photoluminescence lifetime (τ_1 , τ_2 , τ_3 and τ_{av}) of the FWCDs, with and without Fe^{3+} .

	FWCDs	Fe50	Fe100	Fe250
τ_1 (ns)	11.55	11.99	11.93	11.75
τ_2 (ns)	4.19	4.34	4.20	4.26
τ_3 (ns)	1.16	1.20	1.16	1.18
τ_{av} (ns)	2.79	3.14	3.24	3.17

Table 3

Comparison of limit of detection (LOD) and linear detection range for Fe^{3+} of carbon dots prepared from various biomass-based sources.

References	Carbon source	LOD (μM)	Linear detection range (μM)
[10]	Used black tea	0.25	0.25–60
[11]	Sweet potato	0.32	1–100
[12]	Bergamot	0.075	0.025–100
[13]	Silkworm	0.2	1–500
[14]	Sugarcane molasses	1.46	1–100
[15]	Onion waste	0.31	0–20
[16]	Curcumin	0.62	0–6
This work	Hamburger sandwich leftover	32	12.5–100

2. Experimental design, materials and methods

2.1. Synthesis of carbon dots

Cat feed stocks (Catsrang, Dajoo industry) produced from the organic waste were used for the synthesis of CDs along the temperature. The feed stocks were ground to fine powder and dried at 65 °C for 24 h. After the powder was mixed with 50ml distilled water for 7 wt%, hydrothermal carbonization of the source was conducted at 110, 150 and 180 °C for 24 h. The obtained solution was purified by filtering (0.5 μm PTFE membrane) and dialysis (Biotech CD dialysis tubing, 0.5–1.0 kDa, Spectrum Labs.). The carbon dots obtained at 110, 150 and 180 °C were noted as CD110, CD150 and CD180, respectively. Hamburger sandwich leftover was synthesized at 180 °C to food waste-driven carbon dots.

2.2. Selectivity test for Fe³⁺

The all metal salts in this experiment were purchased from Sigma Aldrich. And they was used as received.

For metal quenching test, the all metal salts were dissolved at concentration of 500 μM and mixed with FWCDs solution (10 μg/ml). The PL intensities were measured after 30 min by excitation wavelength of 340 nm.

2.3. Characterization

X-ray photoelectron spectroscopy (XPS, K-alpha, Thermo Scientific) were carried out to characterize the chemical structure of the samples. Fluorescence lifetimes were obtained by the time-correlated single photon counting method (TCSPC, Fluo Time 200 instrument, Picoquant). An excitation source was used 342 nm pulsed LED with repetition rate of 5 MHz. The decay profiles were analyzed by FluoFit Pro software using exponential fitting models through deconvolution with instrumental response functions (IRF).

The PL spectroscopy (FS-2, SICNCO) and UV–vis absorption spectroscopy (Cary 60 UV/vis spectrophotometer, Agilent Technologies) were used for PL properties.

Acknowledgements

This research was supported by the National Research Foundation of Korea funded by the Ministry of Science (NRF-2018R1A2B6003570). This paper was supported by Konkuk University Researcher Fund in 2018.

Transparency document

Transparency document associated with this article can be found in the online version at <https://doi.org/10.1016/j.dib.2019.104038>.

References

- [1] J. Ahn, Y. Song, J.E. Kwon, S.H. Lee, K.S. Park, S. Kim, J. Woo, H. Kim, Food waste driven N-doped carbon dots: applications for Fe³⁺ sensing and cell imaging, *Mater. Sci. Eng. C* 102 (2019) 106–112, <https://doi.org/10.1016/j.msec.2019.04.019>.
- [2] H. Huang, Y. Cui, M. Liu, J. Chen, Q. Wan, Y. Wen, F. Deng, N. Zhou, X. Zhang, Y. Wei, A one-step ultrasonic irradiation assisted strategy for the preparation of polymer-functionalized carbon quantum dots and their biological imaging, *J. Colloid Interface Sci.* 532 (2018) 767–773, <https://doi.org/10.1016/j.jcis.2018.07.099>.
- [3] Q. Wan, Q. Huang, M. Liu, D. Xu, H. Huang, X. Zhang, Y. Wei, Aggregation-induced emission active luminescent polymeric nanoparticles: non-covalent fabrication methodologies and biomedical applications, *Appl. Mater. Today* 9 (2017) 145–160, <https://doi.org/10.1016/j.apmt.2017.06.004>.
- [4] M. Lin, H.Y. Zou, T. Yang, Z.X. Liu, H. Liu, C.Z. Huang, An inner filter effect based sensor of tetracycline hydrochloride as developed by loading photoluminescent carbon nanodots in the electrospun nanofibers, *Nanoscale* 8 (2016) 2999–3007, <https://doi.org/10.1039/C5NR08177G>.

- [5] V. Arul, T.N. Edison, Y.R. Lee, M.G. Sethuraman, Biological and catalytic applications of green synthesized fluorescent N-doped carbon dots using *Hylocereus undatus*, *J. Photochem. Photobiol., B* 168 (2017) 142–148, <https://doi.org/10.1016/j.jphotobiol.2017.02.007>.
- [6] M.-H. Yang, S.-S. Yuan, T.-W. Chung, S.-B. Jong, C.-Y. Lu, W.-C. Tsai, W.-C. Chen, P.-C. Lin, P.-W. Chiang, Y.-C. Tyan, Characterization of silk fibroin modified surface: a proteomic view of cellular response proteins induced by biomaterials, *BioMed Res. Int.* 13 (2014), <https://doi.org/10.1155/2014/209469>.
- [7] Y. Wang, Y. Zhao, F. Zhang, L. Chen, Y. Yang, X. Liu, Fluorescent polyvinyl alcohol films based on nitrogen and sulfur co-doped carbon dots towards white light-emitting devices, *New J. Chem.* 40 (2016) 8710–8716, <https://doi.org/10.1039/C6NJ01753C>.
- [8] J. Coates, Interpretation of Infrared Spectra, a Practical Approach, *Encyclopedia of Analytical Chemistry: Applications, Theory and Instrumentation*, 2006, <https://doi.org/10.1002/9780470027318.a5606>.
- [9] K. Nakason, B. Panyapinyopol, V. Kanokkantapong, N. Viriya-empikul, W. Kraithong, P. Pavasant, Characteristics of hydrochar and liquid fraction from hydrothermal carbonization of cassava rhizome, *J. Energy Inst.* 91 (2018) 184–193, <https://doi.org/10.1016/j.joei.2017.01.002>.
- [10] P. Song, L. Zhang, H. Long, M. Meng, T. Liu, Y. Yin, R. Xi, A multianalyte fluorescent carbon dots sensing system constructed based on specific recognition of Fe(III) ions, *RSC Adv.* 7 (2017) 28637–28646, <https://doi.org/10.1039/c7ra04122e>.
- [11] J. Shen, S. Shang, X. Chen, D. Wang, Y. Cai, Facile synthesis of fluorescence carbon dots from sweet potato for Fe³⁺ sensing and cell imaging, *Mater. Sci. Eng. C* 76 (2017) 856–864, <https://doi.org/10.1016/j.msec.2017.03.178>.
- [12] J. Yu, N. Song, Y.-K. Zhang, S.-X. Zhong, A.-J. Wang, J. Chen, Green preparation of carbon dots by Jinhua bergamot for sensitive and selective fluorescent detection of Hg²⁺ and Fe³⁺, *Sensor. Actuator. B Chem.* 214 (2015) 29–35, <https://doi.org/10.1016/j.snb.2015.03.006>.
- [13] X. Lu, C. Liu, Z. Wang, J. Yang, M. Xu, J. Dong, P. Wang, J. Gu, F. Cao, Nitrogen-doped carbon nanoparticles derived from silkworm excrement as on-off-on fluorescent sensors to detect Fe(III) and biothiols, *Nanomaterials* 8 (2018) 443–454, <https://doi.org/10.3390/nano8060443>.
- [14] G. Huang, X. Chen, C. Wang, H. Zheng, Z. Huang, D. Chen, H. Xie, Photoluminescent carbon dots derived from sugarcane molasses: synthesis, properties, and applications, *RSC Adv.* 7 (2017) 47840–47847, <https://doi.org/10.1039/c7ra09002a>.
- [15] R. Bandi, B.R. Gangapuram, R. Dadigala, R. Eslavath, S.S. Singh, V. Guttena, Facile and green synthesis of fluorescent carbon dots from onion waste and their potential applications as sensor and multicolour imaging agents, *RSC Adv.* 6 (2016) 28633–28639, <https://doi.org/10.1039/c6ra01669c>.
- [16] T. Pal, S. Mohiyuddin, G. Packirisamy, Facile and green synthesis of multicolor fluorescence carbon dots from curcumin: in vitro and in vivo bioimaging and other applications, *ACS Omega* 3 (2018) 831–843, <https://doi.org/10.1021/acsomega.7b01323>.